Metrologia
Fortaleza - CE 2017

High sensitivity GMI gradiometer for measurement of low intensity magnetic fields

P A D Riveros [1], E C Silva [1], C R H Barbosa [2]

[1] Department of Electrical Engineering, Pontifical Catholic University of Rio de Janeiro
[2] Postgraduate Program in Metrology, Pontifical Catholic University of Rio de Janeiro

E-mail: hall@puc-rio.br

Abstract: This paper presents the development of a high sensitivity giant magnetoimpedance (GMI) gradiometer, aimed at measuring ultra-weak magnetic fields. In order to increase the signal-to-noise ratio, the use of gradiometric configurations is mandatory when measuring ultra-weak magnetic fields in unshielded environments. In this work, a first-order GMI gradiometer is designed using two $Co_{70}Fe_5Si_{15}B_{10}$ amorphous ribbon-shaped samples connected to an electronic circuit that converts magnetic field in an output voltage. This paper describes the electronic circuit developed to implement the proposed GMI gradiometer and analyzes its performance by computational simulations.

Keywords: Giant Magnetoimpedance; Magnetic Sensors; Electronic Instrumentation; Gradiometer; High sensitivity.

1. INTRODUCTION

The GMI effect consists in a large change in the complex impedance of a soft ferromagnetic conductor, excited by an alternating current (AC), when subjected to an external magnetic field [1]. GMI transducers have been developed by worldwide researchers and employed in many applications, such as biomedical and biological [2], and aerospace research [3]. The use of GMI sensors in these applications have shown that these new sensing devices have many advantages in relation to conventional magnetic sensing technologies, such as low cost, high sensitivity, wide bandwidth, portability and operability at room temperature [1, 4].

Furthermore, recent researches indicate that GMI magnetometers based on impedance phase readings have significantly higher sensitivities than those based on impedance magnitude readings [5]. However, when it comes to measuring ultra-weak magnetic fields (under 1 nanoTesla), the environmental noise and interference are usually several orders of magnitude larger than the signals of interest. Therefore, such measurements will be significantly affected by spurious components, regardless of the sensitivity of the transducer.

High sensitivity magnetic measurements can be performed inside magnetically shielded rooms, that attenuate magnetic interference by several orders of magnitude [6]. In spite of their effectiveness, shielding solutions are very expensive. On the other hand, a low-cost alternative solution is based on the use of gradiometric configurations, that perform a differential measurement between two identical sensors G_1 and G_2, one close to the magnetic source of interest and the other separated by a proper distance. Since the magnetic interference

in both sensors is almost the same, it is mostly cancelled by differential measurements [7]. Thus, this paper focus on the implementation of GMI gradiometer based on the impedance phase characteristics of two GMI samples.

2. CHARACTERIZATION OF THE GMI SAMPLES

In order to measure the impedance phase characteristics of both sensors, G1 and G2, they have been excited by electrical currents with 15 mA amplitude, 100 kHz frequency and 80 mA DC level. Furthermore, both sensors were subjected to an external DC magnetic field H, longitudinal to their lengths, varying from −2.0 Oe to +2.0 Oe, with 0.1 Oe steps. It should be noted that oersted (Oe) is the unit of the magnetic field H in the CGS system, which is widely used in the GMI effect literature. On the other hand, in the international system of units this same magnitude is expressed in ampere per meter (A/m), and the relation between these units is given by,

$$1\ [Oe] = 10^3/4\pi\ [A.m^{-1}] \qquad (1)$$

The impedance of each GMI sensor $Z_{SENS}(H)$ can be satisfactorily modeled by a resistance $R_{SENS}(H)$ in series with an inductance $L_{SENS}(H)$ [1,5], as given by,

$$Z_{SENS}(H) = R_{SENS}(H) + j\omega\, L_{SENS}(H) \qquad (2)$$

A Helmholtz coil was used to generate the external DC magnetic field and a four-terminal configuration of a precision LCR meter (Agilent, 4285A) was employed to measure the impedance, and also to provide the adequate current to the samples, during the characterization process. Figure 1 presents the schematic diagram of the characterization system, the sample–coil set was positioned in a way to guarantee that the direction of the Earth's magnetic field was transversal to the length of the GMI samples, aiming to reduce its influence on the measurements. The spot welding technique was employed to connect the terminals of the GMI ribbons to the electrical terminals, aiming at the excitation and reading of the GMI samples by the LCR meter. Then, the electrical wires were connected to the electrical terminals using conventional tin–lead solder [8].

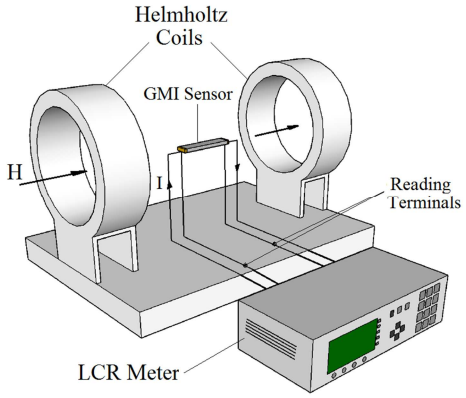

Figure 1. Schematic diagram of the experimental set up used to characterize the GMI samples.

Figure 2 presents the result of the characterization process, showing the impedance phase of the two GMI samples, G1 and G2, as a function of the external magnetic field.

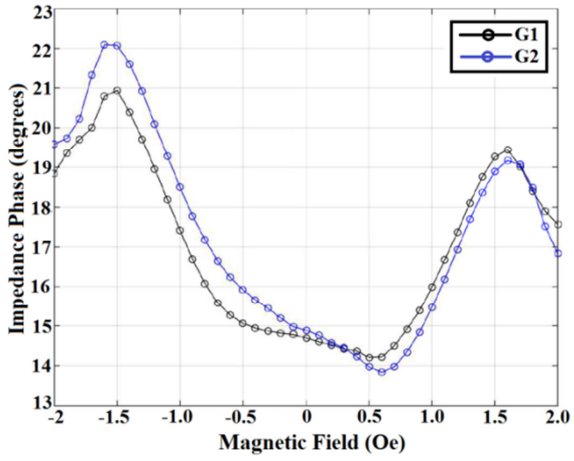

Figure 2. Impedance phase of both GMI samples, G_1 and G_2, as a function of the magnetic field.

Figure 2 indicates the existence of a high sensitivity, about 6.7°/Oe, and satisfactorily

linear region around H = 1.1 Oe. The phase characteristics of both samples are similar within this region, what is extremely important for the gradiometer's performance. Therefore, in order to preserve the linearity of the gradiometer's response, its operating region lies between H = 0.8 Oe and H = 1.4 Oe. The biasing magnetic field was set to H_{pol} = 1.1 Oe, to ensure a symmetrical excursion of the signal through the operating region.

3. GMI GRADIOMETER

The electronic circuit that implements the GMI gradiometer is shown in figure 3. To operate that circuit as a gradiometer, the switches SWA and SWC must be closed, and SWB and SWD must be open. The current used to excite the GMI samples is generated by the association of voltage sources V_{AC} and V_{DC} with the resistors R_A, R_B, R_C and R_D. The AC voltage used to generate the excitation current of the first GMI sensor is in phase with $V_{AC,}$ but the one used to generate the excitation current of the second GMI sensor is 90^o shifted from V_{AC}, due to the phase shifter block.

In turn, after this stage, due to the phase dependency of the GMI samples with the magnetic field, V_A and V_B will be shifted by $\varphi_1(H_{pol})$ and $\varphi_2(H_{pol})$ + 90^o in relation to V_{AC}, respectively. Assuming that both samples have the same phase behavior and are subject to the same magnetic field H_{pol}, the phase shifts introduced by both samples are exactly the same, $\varphi_1(H_{pol}) = \varphi_2(H_{pol})$. Then, at the biasing field (H_{pol}), the voltage V_A will be shifted 90° in relation to V_B. One should notice, however, that this assumption is an idealization that considers that both samples are perfectly homogeneous. Nonetheless, as shown in figure 2, the phase behaviors of the real samples have slight heterogeneities over the operation region.

Since V_A and V_B are composed by an AC component added to a DC level, these signals pass through a high-pass filter that removes their DC components. The outputs of these filters are connected to the inputs of two comparators, working as zero crossing detectors. These comparators convert sinusoidal signals into square waves. Ideally, the phase difference between the signals connected to the comparators inputs is the same to the one measured between their outputs. The XOR block receives two square waves and at its output provides a square wave with a variable duty cycle, proportional to the phase difference of the input signals. Since, at H_{pol}, the inputs of the XOR are 90^o shifted between themselves, the output of the XOR is a square wave with 50% duty cycle and twice the frequency of the signals connected to its inputs.

The XOR output is connected to a low-pass filter, with a cut-off frequency much lower than the frequency of the XOR output signal, therefore extracting the DC component of the input signal, which is proportional to the phase difference of the two samples. In turn, this phase difference is proportional to the magnetic field difference (ΔH), between the two samples. Then, when ΔH = 0 the DC level at the low-pass filter output will be a fixed value, but variations on ΔH will produce voltage variations at the low-pass filter output. Finally, the last stage of the GMI gradiometer consists in an instrumentation amplifier with an offset compensation, in order to obtain an output voltage of zero when ΔH = 0, and also to amplify the low-pass filter output. It's important to point out that in [8], a similar circuit was designed, however, this circuit implemented a magnetometer. Therefore, aiming at improving the signal-to-noise ratio, the electronic circuit proposed in this paper implements not a magnetometer but a gradiometer. In the gradiometer, the output voltage is proportional to the magnetic field difference upon the two GMI sensors.

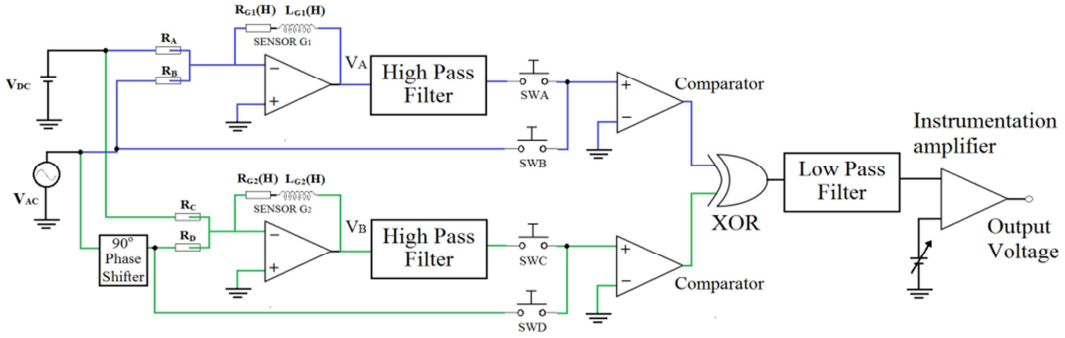

Figure 3. Electronic circuit of the GMI gradiometer. When SWA and SWC are closed the circuit operates as a gradiometer, when SWA and SWD are closed the circuit operates as a magnetometer using sensor G_1, and when SWB and SWC are closed it operates as a magnetometer using sensor G_2.

5. RESULTS

Aiming at evaluating the performance of the electronic circuit of the GMI gradiometer, shown in figure 3, SPICE simulations were performed. In these simulations, both sensors (G_1 and G_2) were electrically modeled by a resistance $R_{SENS}(H)$ in series with an inductance L_{SENS}(H), as defined in equation (2). Figure 3 illustrates the output voltage of the gradiometer, for magnetic field gradients ΔH between -0.3 Oe and +0.3 Oe, in steps of 0.1 Oe. The output voltage as a function of magnetic field gradients is shown in figure 4.

In figure 3 it can be observed a settling time of about 3 ms, mainly due to the low-pass filter stabilization time, and a mean sensitivity of about 10 V/Oe or, equivalently, 100 mV/μT. Furthermore, it can be observed that, for the same variations of ΔH, approximately the same voltage variations are obtained, which indicates that the circuit has a good linearity. Besides, as expected, a zero-voltage output is obtained for a null magnetic field gradient, $\Delta H = 0$. In figure 4, as expected, it can be seen that the circuit output voltages are almost linear for -0,3 Oe < ΔH < +0,3 Oe. It should be noted that figure 4 was obtained from figure 3, considering the steady-state output voltages of the gradiometer.

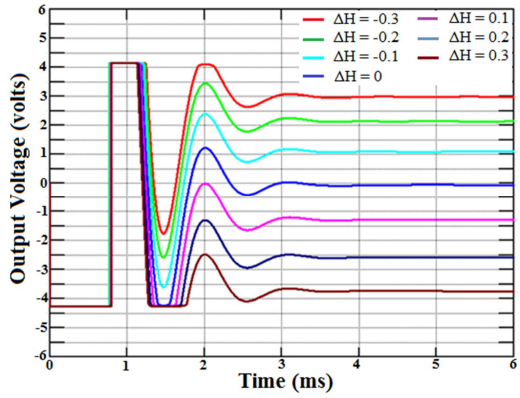

Figure 3. Output voltage of the GMI gradiometer obtained by computational simulations, for different magnetic field gradients ΔH.

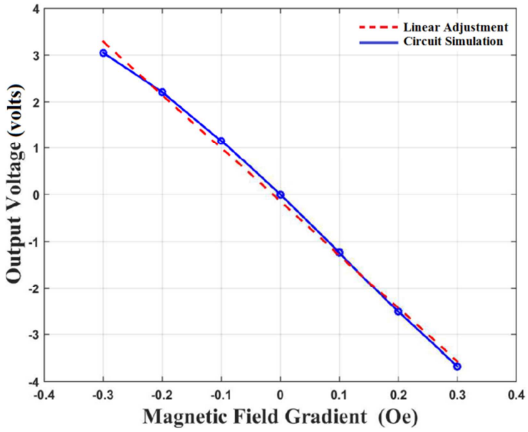

Figure 4. Output voltage of the GMI gradiometer as a function of magnetic field gradients ΔH.

6. CONCLUSIONS

This paper presented the development of a high sensitivity GMI gradiometer for measurements of low intensity magnetic fields in unshielded environments. The proposed electronic circuit for the GMI gradiometer uses the impedance phase characteristics of GMI samples. The circuit was presented and evaluated by computational simulations. As a result, a sensitivity of 100 mV/μT was achieved. It was also noticed that the developed gradiometer presents a good linearity for measurements of magnetic field gradients between ±0.3 Oe or, equivalently, ±30 μT. This behavior was expected, as, for these field gradients, both sensor elements are kept inside their linear regions, from 0.8 Oe and 1.4 Oe.

ACKNOWLEDGMENTS

The authors thank CAPES and CNPq for financial support to the development of this work.

REFERENCES

[1] Phan M H and Peng H X 2008 Giant magnetoimpedance materials: Fundamentals and applications *Prog. Mater. Sci.* **53(2)** 323–420

[2] Kurlyandskaya G V and Miyar F V 2007 Surface modified amorphous ribbon based magnetoimpedance biosensor *Biosensensors and Bioelectronics* **22(9-10)** 2341–5

[3] Lenz J and Edelstein S 2006 Magnetic sensors and their applications *IEEE Sens. J.* **6(3)** 631–49

[4] Mahdi D, Panina A E, Mapps L 2003 Some new horizons in magnetic sensing: high-Tc SQUIDs, GMR and GMI materials *Sensors Actuators A* 105(3) 271–85

[5] Costa Silva E, Gusmão L A P, Hall Barbosa C R and Costa Monteiro E 2014 An enhanced electronic topology aimed at improving the phase sensitivity of GMI sensors *Meas. Sci. Technol.* **25(11)** 115010

[6] Carneiro A A O, Ferreira A, Moraes E R, Araujo D B, Sosa M and Baffa O 2000 Biomagnetism: Instrumental Aspects and Applications *Rev. Bras. Ensino Física* **22(3)** 324–38

[7] Costa Silva E, Hall Barbosa C R, Gusmão L A, Leipner Y, Fortaleza L G, Monteiro E C 2014 Point matching: A new electronic method for homogenizing the phase characteristics of giant magnetoimpedance sensors *Rev. Sci. Instrum.* **85(8)** 084708

[8] Costa Silva E, Hall Barbosa C R, Gusmão L A, Costa Monteiro E, Machado F L A 2011 High sensitivity giant magnetoimpedance (GMI) magnetic transducer: magnitude versus phase sensing *Measurement Science and Technology* **22(3)** 035204